Astronomical and Astrophysical Transactions (*AApTr*), 2025, Vol. 35, Issue 1, pp. 17–28,
ISSN 1055-6796, Photocopying permitted by license only, ©Cambridge Scientific Publishers

Numerical modeling of the influence of the Lidov–Kozai mechanism on the dynamics of near-Lunar objects

N.A. Popandopulo*, V.A. Avdyushev, I.V. Tomilova, T.V. Bordovitsyna

Tomsk State University, Lenin Pr. 36, Tomsk, 634050 Russia

Received 3 April, 2025; accepted 1 May, 2025

This paper presents the results of a numerical analysis of the Lidov–Kozai mechanism's influence on the orbital dynamics of near-lunar objects. We provide estimates of how different perturbing factors affect the timescale of the Lidov–Kozai effect in the objects' orbital evolution. Our study demonstrates that the features of the Lidov–Kozai mechanism, previously established for near-planetary objects within the doubly averaged three-body problem, remain valid in numerical simulations of near-lunar object motion when all gravitational perturbations are accounted for.

Keywords: Lidov–Kozai mechanism; near-lunar objects; orbital evolution; stationary solutions

1 Introduction

The Lidov–Kozai mechanism (Lidov, 1962; Kozai, 1962; Shevchenko, 2017) is embedded in the dynamical structure of hierarchical three-body systems. In such systems, one of the bodies (the external perturbing body) is located at a large distance from the other two (the central and internal perturbed bodies). Under certain conditions, the mechanism manifests in the orbital motion of the perturbed body as significant oscillations of eccentricity and inclination (Lidov–Kozai effect), as well as of the argument of periapsis (Lidov–Kozai resonance).

There is a great terminological diversity in the descriptions of this phenomenon. The work of Japanese authors (Takashi, Katsuhito, 2019) provides a list of names used for this phenomenon: Lidov–Kozai mechanism, effect, resonance, cycle, oscillation. In this paper, we will stick to the term "mechanism" since "resonance" and "effect" seem to be special cases of the Lidov–Kozai mechanism. The use of the terms "cycle" or "oscillation" is unacceptable. The manifestation of the Lidov–Kozai mechanism in reality is not cyclic. We will also show that the mechanism manifests as an oscillatory process far from always.

*Email: nikas.popandopulos@gmail.com

For the purposes of this study, the most relevant research is presented in (Ely, 2005; Ely et al., 2006). The authors developed so-called "frozen" orbits for lunar spacecraft constellations – orbits that maintain their configuration over long periods of time. They also demonstrated that these orbits remain stable even when all perturbing factors are taken into account. Later, Sirwah et al. (2020) studied frozen orbits at medium lunar altitudes. Their results showed that such orbits exhibit only minor variations in eccentricity, while the inclination remains nearly constant.

None of the mentioned works (Ely, 2005; Ely et al., 2006, Sirwah et al., 2020) associates the so-called frozen orbits with the action of the Lidov–Kozai mechanism. However, as we will show below, the appearance of such orbits is a consequence of an object falling into the exact Lidov–Kozai resonance. The goal of the present work is to numerically model various manifestations of the Lidov–Kozai mechanism in the dynamics of near-lunar objects, including those under the influence of the lunar gravitational field.

2 Research methodology

Let us briefly describe the main theoretical results obtained in the framework of the doubly averaged restricted three-body problem (Lidov, 1962; Kozai, 1962). When the external perturbing body moves along a circular orbit, the averaged equations of motion of the perturbed body have a conserved quantity. This quantity is the third component of the orbital angular momentum, known as the Moiseyev–Lidov–Kozai integral. The integral can be expressed in terms of the eccentricity and inclination relative to the orbital plane of the external body by the formula

$$c_1 = \sqrt{1 - e^2}\cos i = \text{const}. \tag{1}$$

The Lidov–Kozai effect is a long-term phenomenon operating on timescales far exceeding the orbital periods of both the inner and outer celestial bodies. This effect is characterized by long-periodic interrelated changes in the eccentricity and inclination of the orbit, which occur with extremely large amplitudes. The larger the initial inclination of the circular orbit of the inner body, the more significant are the perturbations in its orbital parameters. According to the Lidov–Kozai theory, the effect becomes active when the perturbed object's orbital inclination relative to the perturbing body's orbital plane exceeds a critical threshold (Lidov, 1962; Kozai, 1962)

$$i_c = \arccos\sqrt{3/5} \approx 39.2^\circ. \tag{2}$$

In the Lidov–Kozai theory there is also an additional integral which was first obtained by M.L. Lidov himself (Lidov, 1962):

$$c_2 = e^2(2/5 - \sin^2\omega \sin^2 i) = \text{const}. \tag{3}$$

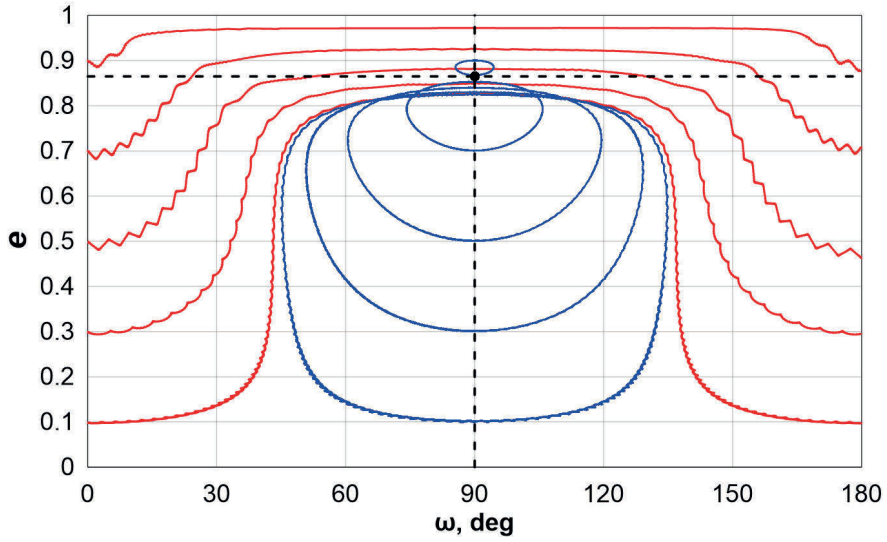


Figure 1 Phase trajectories in the normalized constrained three-body problem under different initial conditions: $a = 1$, $e = 0.1 - 0.9$, $i = 60°$, $\omega = 0°, 90°$. The gravitational parameter of the outer body is $\mu_p = 0.001$, and the radius of its orbit is $a_p = 1.86$. Red lines show the Lidov–Kozai effect (argument of periapsis circulates). Blue lines show the Lidov–Kozai resonance (argument of periapsis displays libration). The point at the intersection of dashed lines corresponds to the exact Lidov–Kozai resonance (stationary solutions).

It is useful because, combined with integral (1), it reduces the study of the Lidov–Kozai mechanism to analyzing phase trajectories in the argument of periapsis–eccentricity plane, parameterized by constants c_1 and c_2 (see Fig. 1).

Although the external body can cause significant perturbations in the orbital elements of the inner body, the Lidov–Kozai theory has stationary solutions (Shevchenko, 2017)

$$a = \text{const},\ \omega = \pm 90°,\ 1 - e^2 = c_1\sqrt{5/3},\ \cos^2 i = c_1\sqrt{3/5}, \tag{4}$$

with a and ω being the semi-major axis and the argument of periapsis of the inner body, respectively. For initial values of the orbital elements close to the stationary state, their solutions display libration. Due to its similarity to librational perturbations observed in orbital resonances (see Fig. 1), this phenomenon is called the Lidov–Kozai resonance, with the stationary solutions referred to as exact Lidov–Kozai resonance. Stationary solutions exist only in the averaged problem where the outer body moves along a circular orbit. However, in more complex practical problems with high-precision modeling, the perturbations in the orbital elements near the stationary solutions (4) turn out to be rather small, which is actually a direct consequence of the theoretical Lidov–Kozai resonance.

Thus, in the present work we define the Lidov–Kozai effect due to the gravitational influence of an external celestial body as significant interrelated non-harmonic

but periodic changes in eccentricity and inclination in the orbital motion of the studied celestial body with an initial circular (or weakly elliptical) but highly inclined orbit. Non-harmonic perturbations of the orbital elements are characterized by a rapid increase in eccentricity and a decrease in inclination to their maximum and minimum values, respectively, followed by a return to their initial values. The inclination decreases to the critical (minimum) value (2), and the maximum values of the orbital elements correspond to their stationary solutions (4).

At the same time, we define the Lidov–Kozai resonance as interrelated libration changes of eccentricity, inclination, and argument of periapsis near their stationary values. However, the Lidov–Kozai mechanism can appear as both an effect and a resonance when all orbital elements display libration with large amplitude (see Fig. 1).

3 Numerical results

Using the original software and mathematical framework developed by the authors (Popandopulo et al., 2022a; Popandopulo et al., 2022b), we conducted an extensive numerical-analytical experiment to study the Lidov–Kozai mechanism in the dynamics of near-lunar objects. The motion of 5,180 objects was simulated over a 10-year period. We examined a family of initial circular orbits with varying semi-major axes a and inclinations i in the selenoequatorial and selenocentric coordinate system. All objects were initialized from the starting position with coordinates $(a, 0, 0)$.

The semi-major axes and orbital inclinations varied within the ranges of $a \in [1.1R_M, 15R_M]$ with a step size of $0.1R_M$ (where R_M is the Moon's radius) and $i \in [0°, 180°]$ with a step size of 5°. The calculations accounted for perturbations caused by the Moon's gravitational field up to the 50th order and degree, as well as the gravitational attraction of the Earth and Sun, treated as point masses. The numerical results were analyzed, and the specific effects of the Lidov–Kozai mechanism on the dynamics of near-lunar objects were identified using the analytical estimates presented in the previous section.

The stability or instability of the resonance was determined by analyzing the behavior of the argument of periapsis according to the following rule (see Fig. 2): libration of the argument of periapsis around $\omega = \pm 90°$ indicates stable resonance, a combination of libration and circulation suggests unstable resonance, while pure circulation indicates the absence of resonance.

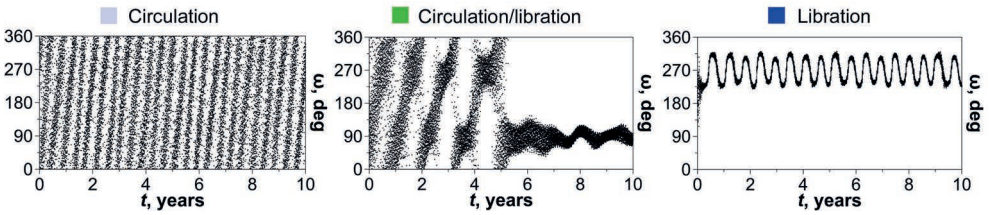


Figure 2 Rules for selecting the type of resonance characteristics and their colour designation on the resonance map.

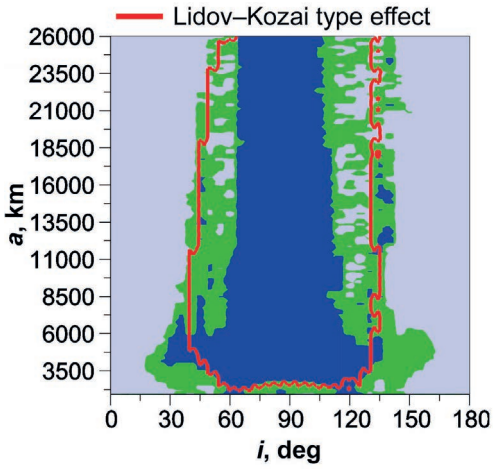


Figure 3 The pattern of behaviour of the argument of periapsis (circulation, circulation/libration, libration) in the dynamics of near-lunar objects depending on the initial values of the large semi-major axis and inclination. The red line shows the boundary of the region where the behaviour of eccentricity and inclination are interrelated in accordance with the Moiseyev–Lidov–Kozai integral (1).

Figure 3 presents a map showing the presence of the Lidov–Kozai resonance in the dynamics of near-lunar objects as a function of initial semi-major axis and inclination values. Notably, in the perturbed problem with initially circular but highly inclined orbits, most objects enter stable resonance despite the argument of periapsis exhibiting nearly chaotic behavior at the initial stage (see Fig. 4). Under these conditions, the Lidov–Kozai effect is particularly strong, with the libration amplitude of the argument of periapsis reaching up to 50°. For initial circular orbits, it is difficult to predict around which of the two stationary values the argument of periapsis will librate, as this depends primarily on the nature of perturbing factors at the simulation onset.

Outside the region of interrelated eccentricity-inclination behavior, the Lidov–Kozai mechanism may manifest as a gradual resonance capture with a relatively weak Lidov–Kozai effect. An example of such resonance is shown in Fig. 4.

Figure 5 demonstrates examples of orbital evolution with developing Lidov–Kozai-type effects, where interrelated eccentricity-inclination behavior is already present but amplitudes remain small. While the Moiseev–Lidov–Kozai integral is conserved, the Lidov integral transitions to negative values. Two model objects were selected with identical orbital elements (a = 5500 km, e = 0.0, i = 41°, ω = 0°, M = 0°) but differing in longitude of ascending node (Ω = 0° and Ω = 270°). These specific longitudes were chosen to illustrate how the Lidov–Kozai effect influences objects with different orbital orientations.

Note that for these objects, the Lidov–Kozai effect manifests differently in the dynamics. When $\Omega = 270°$ the effect occurs faster and with great intensity. At this altitude, such mutual oscillations between eccentricity and inclination lead to the fall of the object in about 6.5 years (Figs. 5b, 5d, and 5f, graphs marked in green).

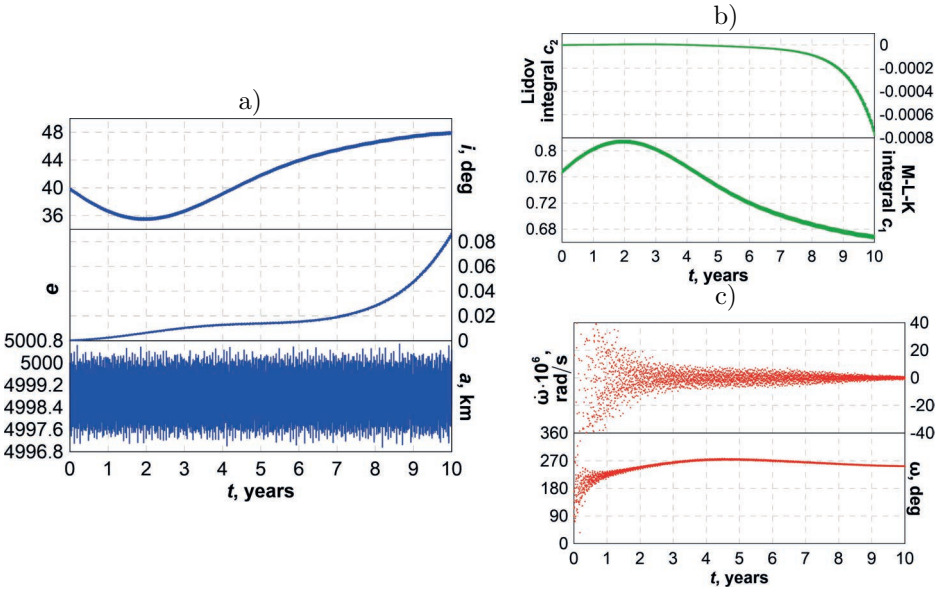


Figure 4 Example of a weak Lidov–Kozai-type resonance with perturbations from the full gravitational field of the Moon, Sun and Earth: a) Orbital evolution (top to bottom) of elements i, e, and a; b) Dynamics (top to bottom) of the Lidov integral and Moiseev–Lidov–Kozai integral; c) Evolution (top to bottom) of the resonant argument $\dot{\omega}$ and critical argument ω.

A key feature of near-lunar object dynamics is that, in addition to perturbations from external bodies driving the Lidov–Kozai mechanism, they are also affected by the non-sphericity of the central body. As Fig. 5 demonstrates, lunar oblateness (red curve) and the Moon's full gravitational field (blue curve) partially suppress the pure Lidov–Kozai-type effect (green curve). Notably, when the full gravitational field of the Moon is taken into account in the lunar satellite motion, the Lidov–Kozai-type effect emerges earlier in its dynamical evolution (blue curve).

Figure 6 shows examples of a fully formed Lidov-Eozai effect. The disturbances from the moon's oblateness and the attraction of the Earth and the Sun are taken into account.

Next, we examine the behavior of orbital elements in numerical simulations of lunar satellite motion near stationary solutions. These solutions arise in the doubly averaged restricted three-body problem, where the external perturbing body moves along a circular orbit. If stationary solutions do not exist in the perturbed problem, how small are the deviations around them?

To investigate this, we performed numerical simulations of object motion over a 10-year period with the following initial parameters: $a/R_M \in \{4, 6, 8, 10\}$, $e \in [0.0, 0.7]$, $i \in [40°, 65°]$, $\Omega \in \{0°, 60°, 120°, 180°, 240°, 300°\}$, and $\omega \in \{90°, 270°\}$. Square brackets denote a range, and curly brackets denote a set of values. The orbital evolution of lunar satellites was modeled in a special coordinate system associated with Earth's orbital plane (Carosi et al., 2021). This system was chosen because: (1) Earth's gravity is the dominant factor in the Lidov–Kozai mechanism for near-lunar

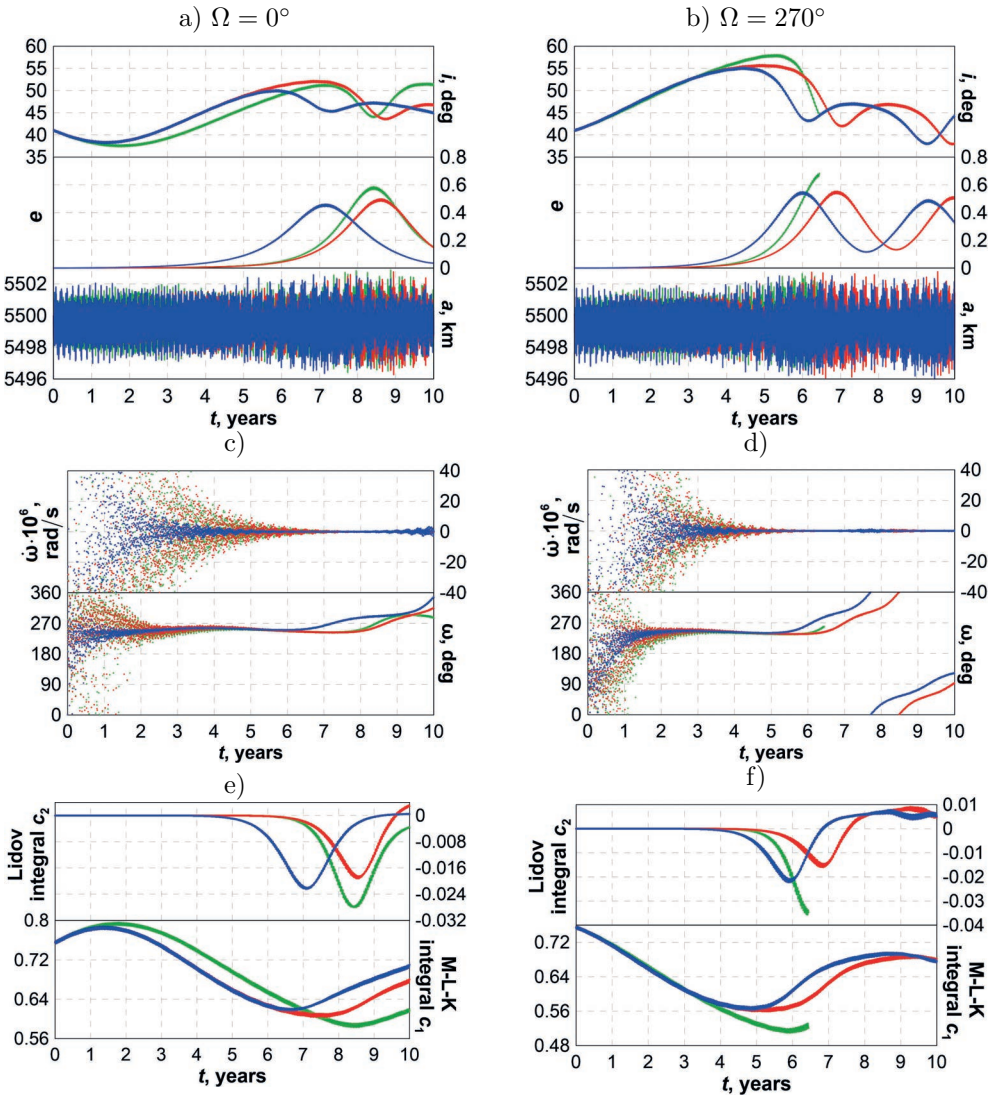


Figure 5 Example of a Lidov–Kozai-type effect under different perturbation regimes: (Blue) Full gravitational field of Moon, Earth and Sun; (Red) Lunar oblateness and gravitation of the Earth and Sun; (Green) Earth and Sun gravitation only. Orbital evolution (top to bottom) of i, e, a for: a) $\Omega = 0°$, b) $\Omega = 270°$. Variation (top to bottom) of Lidov and Moiseev–Lidov–Kozai integrals at c) $\Omega = 0°$, d) $\Omega = 270°$. Evolution (top to bottom) of resonant relation $\dot{\omega}$ and critical argument ω at: e) $\Omega = 0°$, f) $\Omega = 270°$.

objects, while (2) in Lidov–Kozai theory, the orbital plane of the external celestial body serves as the fundamental plane of the coordinate system.

Figure 7 displays four composite plots, each containing six individual maps. Above each composite plot, the initial semi-major axis value used to generate the maps is indicated, while each individual map is labeled with its corresponding initial argument

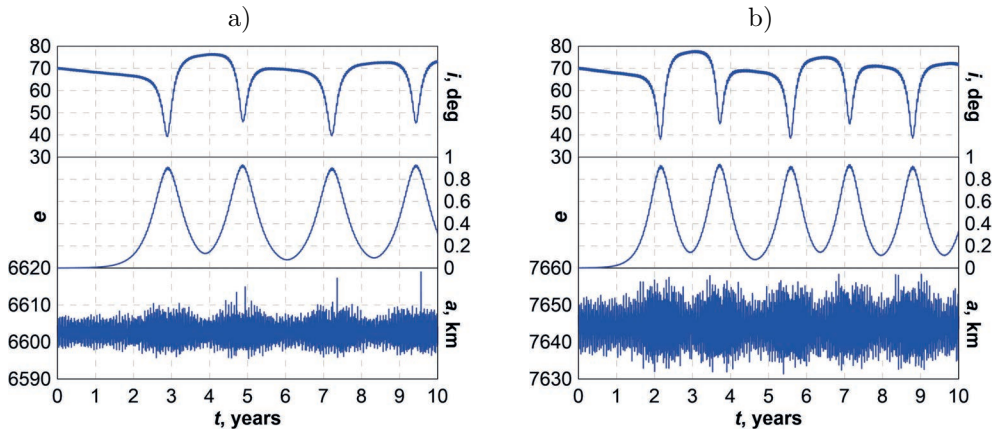


Figure 6 Examples of a fully formed Lizhov–Kozai effect. The disturbances from the Moon's oblateness and the influence of the Earth's and Sun's gravity are taken into account.

of periapsis and longitude of the ascending node. The gradient maps illustrate the dependence of the maximum oscillation amplitude of the orbital argument of periapsis ($\Delta\omega_{max}$) on inclination i and eccentricity e parameters. For analytical convenience, each gradient level on the maps is accompanied by its corresponding numerical value, representing the maximum deviation of ω from its initial value over the 10-year period. Each map features a dashed line marking the curve of stationary solutions from Lidov–Kozai theory (4).

The results presented in Fig. 7 demonstrate that within the selected ranges of inclination and eccentricity, stability regions exist where the maximum oscillation amplitude of the argument of periapsis remains below 20° for $a = 4R_M$, while for higher orbits it reaches up to 30°. The data also reveal that minor variations in the argument of periapsis are characteristic of more inclined and elliptical orbits across all considered semi-major axis values. However, as orbital altitude increases, the regions with minimal perturbations in the argument of periapsis become more constrained.

Table 1 presents additional results for assessing the stability of other orbital parameters. It displays the minimum values of maximum oscillation amplitudes for orbital elements – eccentricity (Δe_{max}), inclination (Δi_{max}), and argument of periapsis ($\Delta\omega_{max}$) – calculated for lunar satellites over a 10-year period. These values were obtained through numerical simulations using the same initial parameter combinations $\{a, e, i, \Omega, \omega\}$ as in Fig. 7, aiming to identify conditions where the maximum oscillations of all three elements $\{e, i, \omega\}$ reach their smallest possible magnitudes. In other words, the table reveals optimal initial orbital configurations that provide the highest stability for these parameters. While Fig. 5 illustrates behavior solely for the argument of periapsis, Table 1 provides specific numerical values demonstrating stability not only in the argument of periapsis but also in eccentricity and inclination.

Analysis of Table 1 data reveals that oscillation amplitudes of the evaluated orbital parameters increase with growing semi-major axis, indicating reduced stability of satellite orbits at higher altitudes. Conversely, lower orbits exhibit minimal oscillations, particularly under specific initial conditions, making them potentially suitable

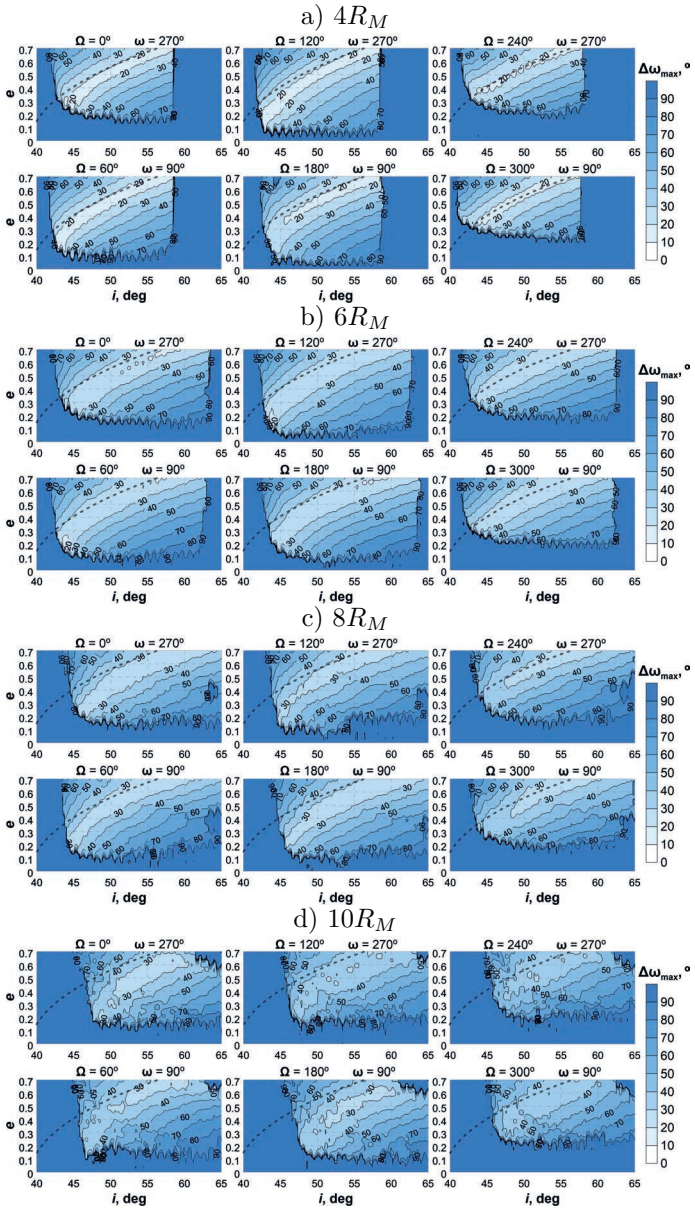


Figure 7 Numerical simulation results showing the oscillation amplitude of the argument of periapsis as a function of initial orbital parameters for semi-major axes of: a) $4R_M$, b) $6R_M$, c) $8R_M$, d) $10R_M$ (see main text for complete details).

for long-term stable trajectories. In regions with minimal orbital parameter oscillations, we observe proximity to stationary solutions of the Lidov–Kozai mechanism (see Fig. 7), confirming that the identified stable orbits correspond to exact Lidov–

Table 1 Estimating the maximum fluctuation amplitudes of the parameters e, i and ω over 10 years in orbits close to stationary solutions.

a, R_M	ω,°	Ω,°	i,°	e	$\Delta\omega_{max}$,°	Δe_{max}	Δi_{max},°
4	90	60	57.2	0.700	14.9	0.025	9.6
		180	57.4	0.700	14.0	0.038	9.3
		300	57.0	0.700	10.0	0.040	12.3
	270	0	57.0	0.700	15.4	0.030	9.0
		120	57.2	0.700	8.6	0.029	12.9
		240	57.0	0.700	14.3	0.039	9.9
6	90	60	57.2	0.700	17.0	0.038	10.4
		180	58.0	0.700	15.6	0.049	9.6
		300	57.6	0.700	12.1	0.046	13.1
	270	0	57.4	0.700	17.2	0.042	9.7
		120	57.4	0.700	11.1	0.041	13.7
		240	57.6	0.700	15.8	0.047	11.0
8	90	60	56.0	0.665	18.9	0.053	11.1
		180	56.6	0.630	17.1	0.076	9.1
		300	57.8	0.700	13.8	0.073	14.1
	270	0	58.8	0.700	17.9	0.063	10.4
		120	58.4	0.700	13.6	0.060	14.2
		240	56.0	0.665	17.6	0.069	11.0
10	90	60	56.8	0.700	14.7	0.058	11.6
		180	58.4	0.630	20.4	0.064	8.9
		300	57.2	0.700	19.8	0.081	14.8
	270	0	58.4	0.630	15.6	0.042	9.7
		120	57.2	0.700	16.5	0.074	13.4
		240	57.0	0.700	21.5	0.080	11.0

Kozai resonance (see Table 1). Optimal eccentricity values for all considered orbits cluster around 0.7, while inclinations fall within the $56° - 58°$ range. According to conditions (4), such orbits satisfy resonance criteria by minimizing changes in both inclination and eccentricity while maintaining a stable argument of periapsis.

Figure 8 presents an example of orbital evolution demonstrating the effects of exact Lidov–Kozai resonance (initial elements: $a = 10428$ km, $e = 0.7$, $i = 57.4°$, $\Omega = 120°$, $\omega = 270°$, $M = 0°$). The left panel shows time variations of parameters

$$L_1 = c_1\sqrt{5/3} - (1 - e^2),\ L_2 = c_1\sqrt{3/5} - \cos^2 i,$$

derived from the stationary solution conditions (4). As evident from Fig. 7c, the quantities L_1 and L_2 oscillate around zero, confirming that the selected orbital parameters closely approximate stationary solutions. The plots in Figs. 7b and 7d further verify the presence of exact Lidov–Kozai resonance in the lunar satellite's orbital dynamics.

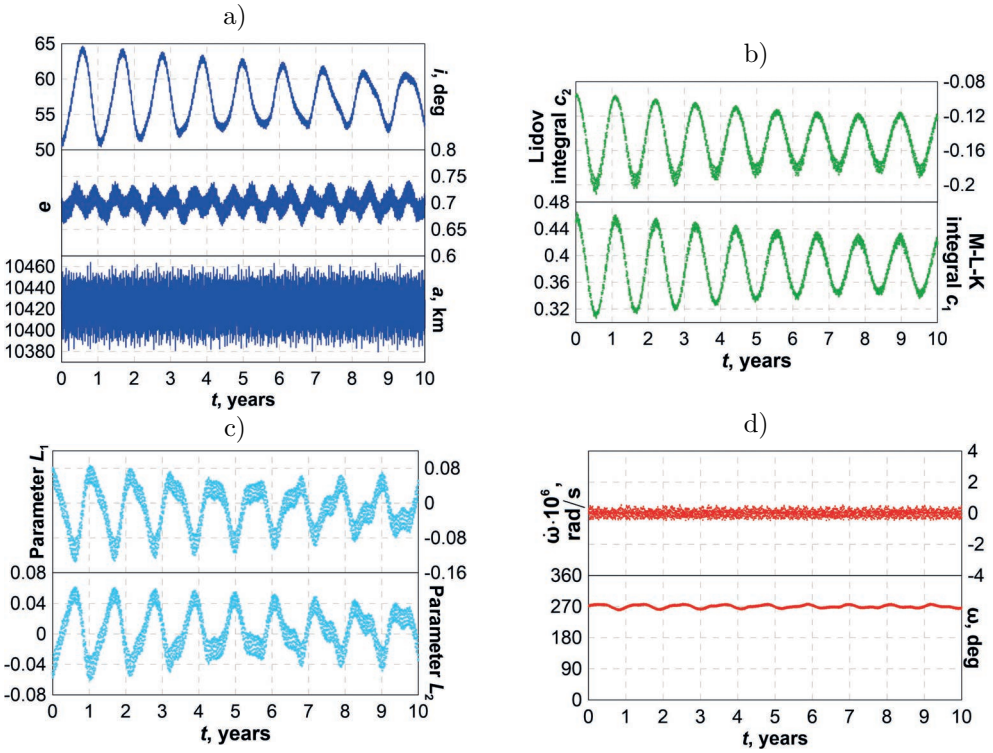


Figure 8 Example of orbital evolution corresponding to a stationary solution: a) Orbital evolution (top to bottom) of elements i, e, and a; b) Time variation (top to bottom) of the Lidov and Moiseev–Lidov–Kozai integrals; c) Time variation (top to bottom) of stationary solution parameters L_1 and L_2 (see text for details); d) Evolution (top to bottom) of the resonant relationship $\dot{\omega}$ and critical argument ω.

Conclusions

The numerical-analytical modeling results of near-lunar object dynamics presented in this study demonstrate that the Lidov–Kozai mechanism manifests in three distinct ways: as a weak Lidov–Kozai resonance; as a Lidov–Kozai effect; through stationary solutions that enable long-term orbital stabilization. Of particular practical interest are orbits approximating stationary solutions, which can be identified for any semi-major axis value through careful selection of eccentricity and inclination, while maintaining the argument of periapsis near $\omega = \pm 90°$. Such orbits near Lidov–Kozai stationary solutions were obtained in studies (Ely, 2005; Ely et al., 2006; Sirwah et al., 2020) and designated as “frozen” orbits.

ACKNOWLEDGEMENTS

The research was carried out within the state assignment of the Ministry of Science and Higher Education of the Russian Federation (theme No. FSWM-2024-0005).

This research was supported in part through computational resources of the supercomputer "SKIF Cyberia" of Tomsk State University.

References

Carosi M., Capolicchio J., Tosti M., Eleuter M., Stallo C., Musacchio D., Di Lauro C. (2021) Joint 26th Ka and Broadband Communications Conference and the 38th International Communications Satellite Systems Conference.

Ely T.A. (2005) The Journal of the Astronautical Sciences, 53(3), 301

Ely T.A., Lieb E. (2006) The Journal of the Astronautical Sciences, 54(1), 53

Kozai Y. (1962) Astron. J, 67, 591

Lidov M.L. (1962) PSS, 9, 719

Popandopulo N.A., Aleksandrova A.G., Tomilova I.V., Avdyushev V.A., Bordovitsyna T.V. (2022a) SSR, 56, 252

Popandopulo N.A., Aleksandrova A.G., Bordovitsyna T.V. (2022b) RPJ, 65, 959

Shevchenko I.I. (2017) Springer. 2017. 198 p.

Sidorenko V.V. (2017) Celest. Mech. & Din. Astr, 130, 4

Sirwah M., Tarek D., Radwan M., Ibrahim A. (2020) Results in Physics, 17, 103

Ito, T. and K. Ohtsuka (2019) The Lidov–Kozai oscillation and Hugo von Zeipel, Monogr. Environ. Earth Planets, 7, 1